Hindawi
Advances in Condensed Matter Physics
Volume 2022, Article ID 8993349, 6 pages
https://doi.org/10.1155/2022/8993349

Research Article

Enhanced Light Emission from Type-II Red InGaN/GaNSb/GaN Quantum-Well Structures

Seoung-Hwan Park,[1] Jong-In Shim,[2] and Dong-Soo Shin[2]

[1]*Department of Electronics Engineering, Catholic University of Daegu, Hayang, Kyeongbuk, Kyeongsan 38430, Republic of Korea*
[2]*Department of Photonics and Nanoelectronics and BK21 FOUR ERICA-ACE Center, Hanyang University ERICA, Ansan, Gyeonggi 15588, Republic of Korea*

Correspondence should be addressed to Dong-Soo Shin; dshin@hanyang.ac.kr

Received 23 May 2022; Accepted 11 August 2022; Published 26 September 2022

Academic Editor: Da-Ren Hang

Electronic and optical properties of type-II InGaN/GaNSb/GaN quantum-well (QW) structures are investigated by using the multiband effective mass theory for potential applications in red light-emitting diodes. The heavy-hole effective mass around the topmost valence band is not affected much by the insertion of the GaNSb layer, and the optical matrix elements are greatly increased by the inclusion of the GaNSb layer in the InGaN/GaN QW structure. As a result, the type-II InGaN/GaNSb/GaN QW structure shows a much larger emission peak than the conventional type-I QW structure owing to the decrease in spatial separation between electron and hole wavefunctions, in addition to the reduction of the effective well width. It is also observed that the In content in InGaN well can be significantly reduced for the type-II QW structure with a large Sb content, compared to that for the type-I QW structure.

1. Introduction

III-nitride-based white light-emitting diodes (LEDs) have received much attention for their tremendous potential for energy-efficient general illumination applications [1–3]. They have been usually fabricated by using InGaN/GaN quantum wells (QWs) as InGaN has a direct band gap covering the entire visible spectrum. So far, blue and green InGaN/GaN LEDs have been improved greatly although the efficiency of green LEDs is still inferior to that of blue LEDs. On the other hand, emission in the red wavelength range typically exhibits much lower quantum efficiency because higher In content and relatively thicker QWs are necessary. [4] The high In content in the QW region leads to the large piezoelectric (PZ) and spontaneous (SP) polarization fields [5, 6], which significantly reduce the internal quantum efficiency of the QW owing to a larger spatial separation between electron and hole wavefunctions.

As a method to reduce the internal field effect, type-II QW structures have been studied by several research groups. The structures considered include the type-II InGaN/GaNAs QW [7, 8], the type-II InGaN/$ZnGeN_2$ QW [9], and the type-II InGaN/$ZnSnN_2$/GaN QW [10, 11]. In addition, the type-II InGaN/GaNSb/GaN QW was proposed to improve the internal quantum efficiency of the InGaN/GaN QW structure for the blue wavelength range [12]. On the other hand, in the case of the red wavelength range, there has been no work reported on the optical properties of the type-II QW structures combining InGaN and GaNSb.

In this paper, we theoretically investigate the electronic and optical properties of the type-II QW structure combining $In_xGa_{1-x}N$ and $GaN_{1-y}Sb_y$ as one way of improving the internal quantum efficiency of the red $In_xGa_{1-x}N$/GaN QW structure. The multiband effective mass theory is utilized to calculate the optical properties of these InGaN/GaNSb/GaN QW structures. The finite difference method (FDM) is implemented in Fortran codes to calculate the valence-band structures. These results are compared with those of the conventional red InGaN/GaN QW structure. The self-consistent (SC) band structures and wavefunctions

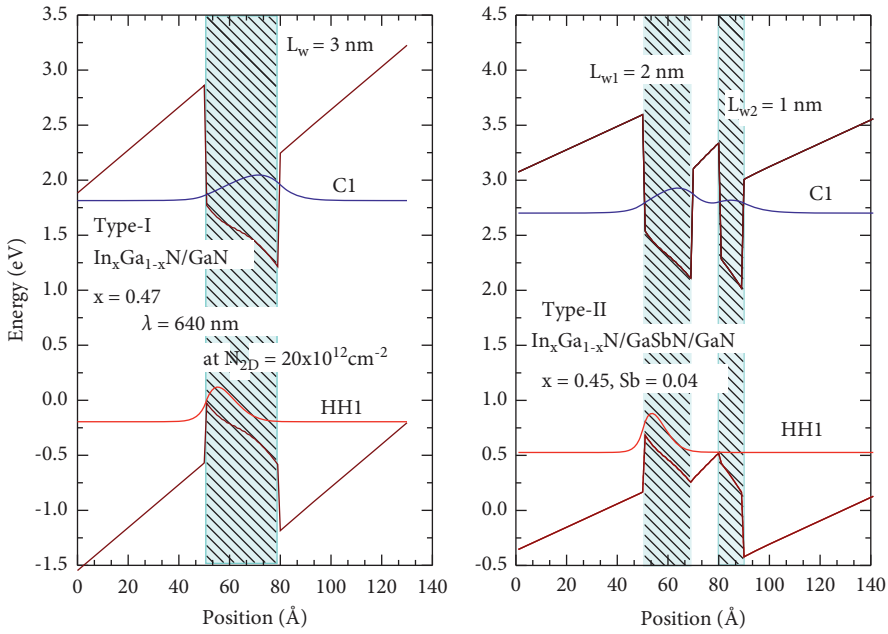

FIGURE 1: Potential energy profiles for (a) type-I $In_xGa_{1-x}N/GaN$ ($x = 0.47$) and (b) type-II $In_xGa_{1-x}N/GaN_{1-y}Sb_y/GaN$ ($x = 0.45$, $y = 0.04$) QW structures. The wavefunctions of the first conduction subband (C1) and the first valence subband (HH1) at the zone center are also shown as blue and red lines, respectively.

are obtained by solving the Schrödinger equation for electrons, the 3×3 Hamiltonian for holes, and the Poisson's equation iteratively [13, 14]. The non-Markovian free-carrier model with bandgap renormalization to calculate the spontaneous emission spectrum $g_{sp}(\omega)$ is taken from [15] and [16]. The bandgap energy of $GaN_{1-y}Sb_y$ used in the calculation is obtained by $E_g^{GaNSb}(y) = yE_g^{GaSb} + (1-y)E_g^{GaN} - Cy(1-y)$, where E_g^{GaSb} and E_g^{GaN} are bandgap energies of GaSb and GaN, respectively, and C is the bowing parameter. Here, we assume that the unknown parameters of GaNSb are same as those of GaN as a first approximation. The material parameters for GaN and InN used in the calculation are taken from [17] and references therein.

2. Results and Discussion

Figure 1 shows potential energy profiles where Figure 1(a) is for the type-I In_x $Ga_{1-x}N/GaN$ QW structure and Figure 1(b) is for the type-II $In_xGa_{1-x}N/GaN_{1-y}Sb_y/GaN$ QW structure. The wavefunctions of the first conduction subband (C1) and the first valence subband (HH1) at the zone center are also shown. The well width of the type-I InGaN/GaN QW structure is fixed as $L_w = 3$ nm. The sum of the left (L_{w1}) and right (L_{w2}) side well widths of the type-II InGaN/GaNSb/GaN QW structure is also selected to be 3 nm. The thickness and the Sb content of the GaNSb layer are set to be 1 nm and 0.04, respectively. The In contents in $In_xGa_{1-x}N$ wells are selected to give a transition energy corresponding to a wavelength of 640 nm, which are 0.47 and 0.45 for the type-I and type-II QW structures, respectively.

In the case of the conventional type-I QW structure, a large spatial separation between electron and hole wavefunctions is observed due to the large internal field. On the other hand, a spatial separation between electron and hole wavefunctions in the type-II InGaN/GaNSb/GaN QW structure is greatly reduced, compared to that of type-I QW structure. Thus, we expect that the optical transition probability will be greatly improved with the inclusion of the GaNSb layer, as discussed in the following.

Figure 2 shows the valence-band structures where Figure 2(a) is for the type-I InGaN/GaN QW and Figure 2(b) is for the type-II InGaN/GaNSb/GaN QW, considered in Figure 1. The SC solutions are obtained at a sheet carrier density of $N_{2D} = 20 \times 10^{12}\text{cm}^{-2}$. The heavy-hole effective mass around the topmost valence band is not affected much by the GaNSb layer. The overall shapes of the valence-band structures for both cases are similar to each other. However, the energy spacing between the first two subbands and the third two subbands of the type-II QW structure is slightly smaller than that of the type-I QW structure.

Figure 3 shows transverse-electric (TE)-polarized optical matrix elements where Figure 3(a) is for the type-I InGaN/GaN QW and Figure 3(b) is for the type-II InGaN/GaNSb/GaN QW as a function of $k_{\|}$ at sheet carrier densities of $2\times$ and $20 \times 10^{12}\text{cm}^{-2}$. Here, we use $2\times$ and $20 \times 10^{12}\text{cm}^{-2}$ as examples of relatively low and high sheet carrier densities. TE-polarized optical matrix elements are shown to be nearly independent of the in-plane wave vector $k_{\|}$ for both QW structures. In the case of the low sheet carrier density, the

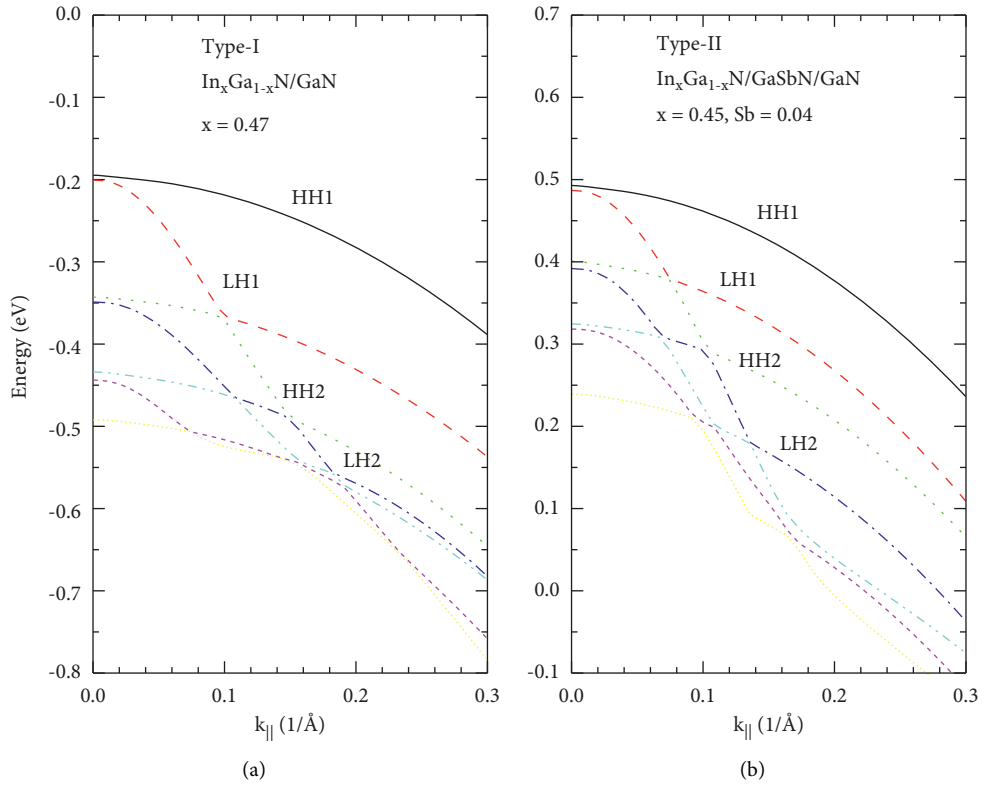

FIGURE 2: Valence-band structures for (a) type-I $In_xGa_{1-x}N/GaN$ ($x = 0.47$) and (b) type-II $In_xGa_{1-x}N/GaN_{1-y}Sb_y/GaN$ ($x = 0.45$, $y = 0.04$) QW structures.

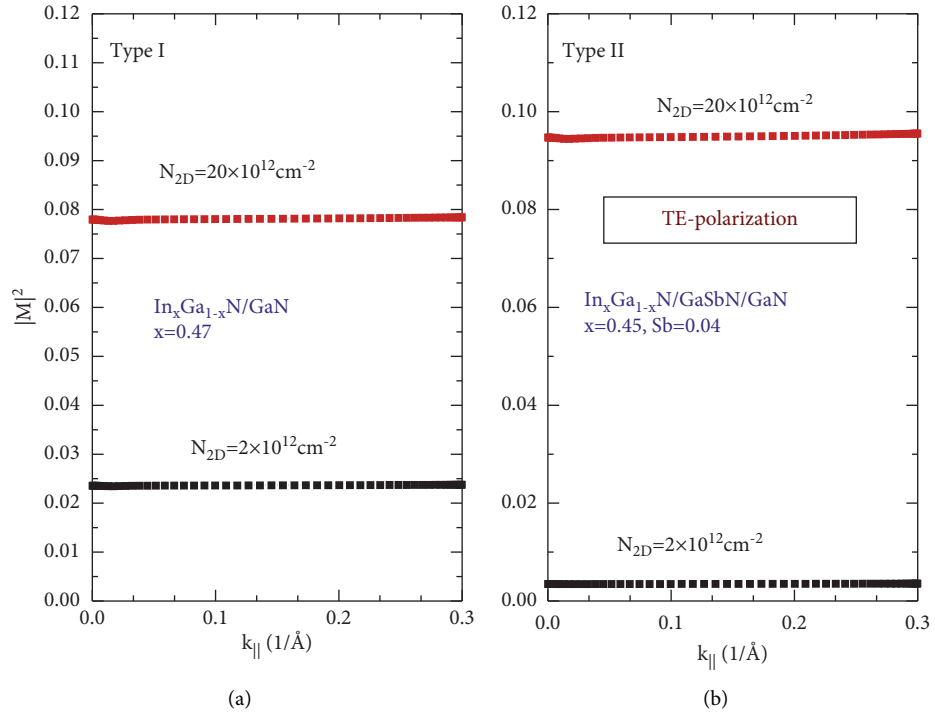

FIGURE 3: TE-polarized optical matrix elements for (a) type-I $In_xGa_{1-x}N/GaN$ ($x = 0.47$) and (b) type-II $In_xGa_{1-x}N/GaN_{1-y}Sb_y/GaN$ ($x = 0.45$, $y = 0.04$) QW structures as a function of $k_{\|}$ at sheet carrier densities of 1× and $20 \times 10^{12}cm^{-2}$.

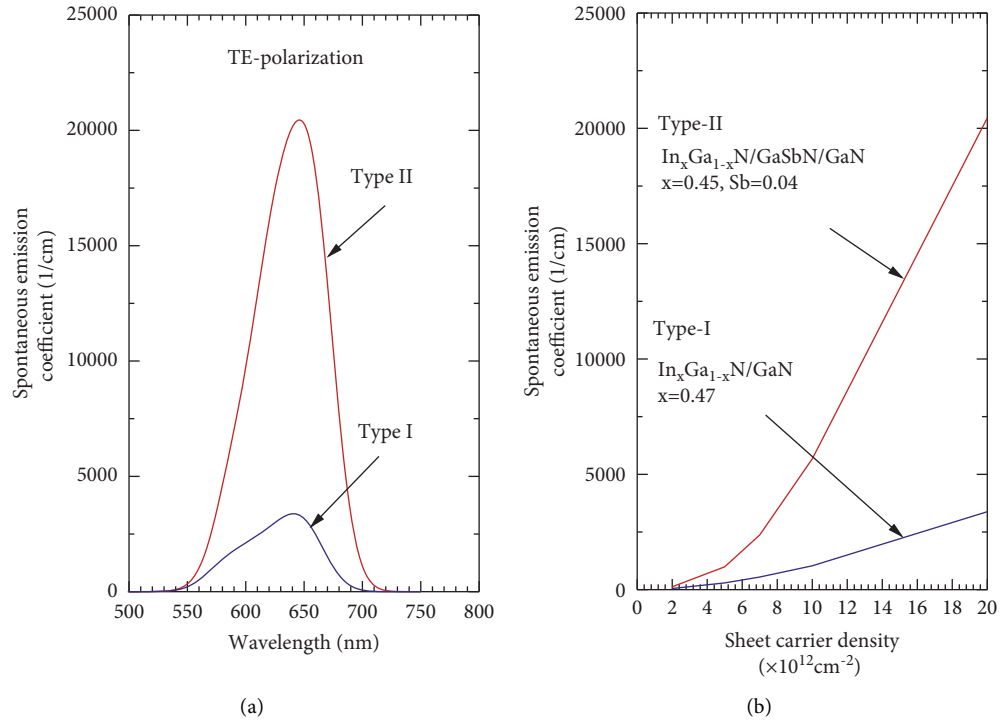

FIGURE 4: (a) TE-polarized spontaneous emission spectra and (b) peak intensities as a function of sheet carrier density for type-I $In_xGa_{1-x}N/GaN$ and type-II $In_xGa_{1-x}N/GaN_{1-y}Sb_y/GaN$ ($x = 0.45$, $y = 0.04$) QW structures.

matrix element of the type-II InGaN/GaNSb/GaN QW structure is shown to be smaller than that of the conventional type-I QW structure. However, at the higher sheet carrier density, the type-II InGaN/GaNSb/GaN QW structure shows a larger matrix element than the conventional type-I QW structure because the reduction effect in the built-in potential by the carrier screening is dominant for the type-II QW structure.

Figure 4 shows TE-polarized spontaneous emission spectra (Figure 4(a)) and peak intensities as a function of sheet carrier density (Figure 4(b)) for type-I InGaN/GaN and type-II InGaN/GaNSb/GaN QW structures. TE-polarized spontaneous emission spectra are obtained at a sheet carrier density of $20 \times 10^{12}\text{cm}^{-2}$. The peak wavelengths of both QW structures are shown to be approximately 640 nm. The type-II InGaN/GaNSb/GaN QW structure shows a larger emission peak than the conventional type-I QW structure in the investigated range of sheet carrier densities although the matrix element of the type-II InGaN/GaNSb/GaN QW structure is smaller than that of the conventional type-I QW structure in the range of low sheet carrier densities owing to a small screening effect. This is mainly because the density of states $k_\parallel/(\pi L_w^{\text{eff}})$ for the type-II QW structure is enhanced owing to the reduction of the effective well width, L_w^{eff}. The effective well width is given by $L_w^{\text{eff}} = [m^c_{w2}(L_{w2} + L'_{w2})/2 + m^v_{w1}L_{w2}]/(m^c{}_{w2} + m^v{}_{w1})$, where m^v_{w1} and m^c_{w2} are hole and electron effective masses for wells, respectively [18].

In particular, in the range of higher sheet carrier densities, the peak intensity of the type-II InGaN/GaNSb/GaN QW structure is much larger than that of the conventional type-I QW structure owing to an increased matrix element. Also, the peak intensities of both QW structures rapidly increase with increasing sheet carrier density. The increasing rate of the peak intensity for type-II QW structure is larger than that for type-I QW structure. If the Sb content in GaNSb is increased, the In content in InGaN well can be significantly reduced, as discussed in the following.

Figure 5 shows the potential energy profile for the type-II $In_xGa_{1-x}N/GaN_{1-y}Sb_y/GaN$ QW structure with $x = 0.3$ and $y = 0.08$ (Figure 5(a)) and TE-polarized spontaneous emission spectra of both type-I and type-II QW structures (Figure 5(b)). The inset in Figure 5(b) shows the TE-polarized optical matrix element for the type-II $In_xGa_{1-x}N/GaN_{1-y}Sb_y/GaN$ QW structure ($x = 0.3$, $y = 0.08$). The SC solutions are obtained at a sheet carrier density of $20 \times 10^{12}\text{cm}^{-2}$. The thickness of the GaNSb layer is set to be 1 nm as in Figure 1, but the Sb content of the GaNSb layer is changed from 0.04 to 0.08. With this change, the transition wavelength of 640 nm is obtained at an In content of 0.3 in the InGaN well. This value is much smaller than that for the type-I $In_xGa_{1-x}N/GaN$ QW structure ($x = 0.47$). In addition, we observe that the type-II InGaN/GaNSb/GaN QW structure still has a much larger emission peak than the conventional type-I QW structure even for the case of

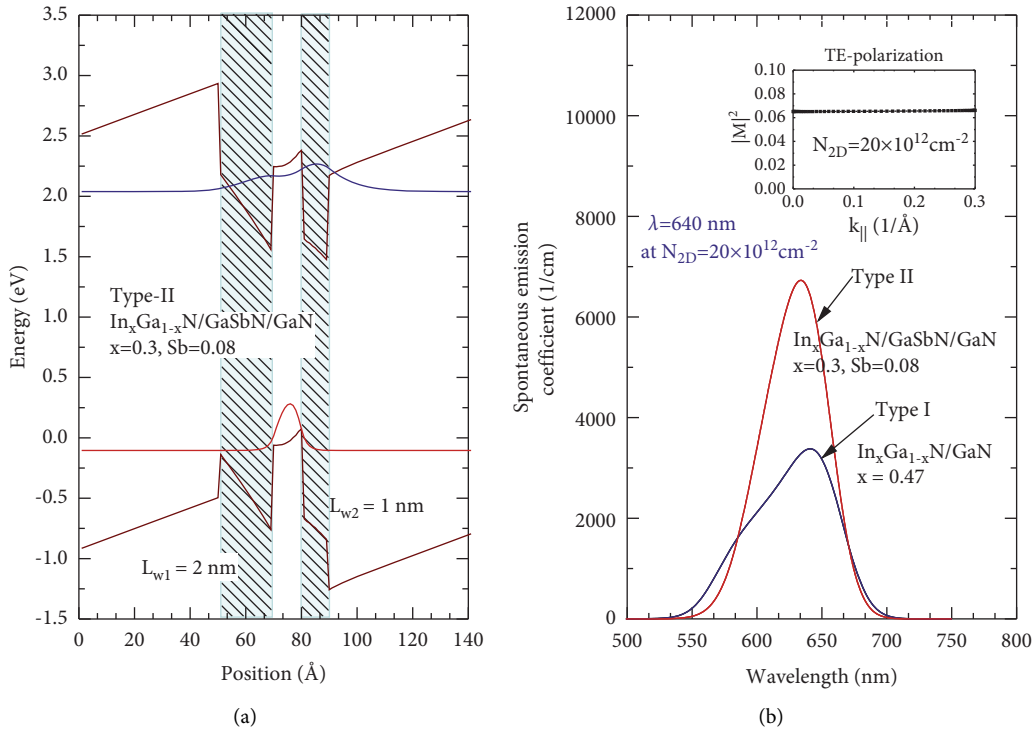

FIGURE 5: Potential energy profile for (a) the type-II $In_xGa_{1-x}N/GaN_{1-y}Sb_y/GaN$ QW structure ($x = 0.3$ and $y = 0.08$) and (b) TE-polarized spontaneous emission spectra of both the type-I and type-II QW structures. The inset shows the TE-polarized optical matrix element for the type-II $In_xGa_{1-x}N/GaN_{1-y}Sb_y/GaN$ QW structure ($x = 0.3$, $y = 0.08$).

smaller In content. On the other hand, the emission peak of the type-II $In_xGa_{1-x}N/GaN_{1-y}Sb_y$ /GaN QW structure ($x = 0.3$, $y = 0.08$) is slightly smaller than that of the type-II $In_xGa_{1-x}N/GaN_{1-y}Sb_y/GaN$ QW structure ($x = 0.45$, $y = 0.04$) because the former has a smaller optical matrix element than the latter owing to the reduced overlap between electron and hole wavefunctions.

3. Summary

In summary, electronic and optical properties of type-II red InGaN/GaNSb/GaN QW structure have been investigated by using the multiband effective mass theory. Optical matrix elements for the type-II InGaN/GaNSb/GaN QW structures are greatly increased owing to the screening effect with increasing sheet carrier density. The type-II InGaN/GaNSb/GaN QW structures show much larger emission peaks than the conventional type-I QW structure in an investigated range of sheet carrier densities because the density of states for the type-II QW structure is enhanced owing to the reduction of the effective well width. Also, we have observed that the In content in InGaN well can be significantly reduced with increasing Sb content in the GaNSb layer.

Data Availability

The data used to support the findings of this study are available from the corresponding author upon request.

Conflicts of Interest

The authors declare that they have no conflicts of interest.

Acknowledgments

This research was supported by the Nano Material Technology Development Program through the National Research Foundation of Korea (NRF) funded by the Ministry of Science and ICT (Grant 2021M3D1A2048623).

References

[1] B. Jain, R. T. Velpula, H. Q. Thang Bui et al., "High performance electron blocking layer-free InGaN/GaN nanowire white-light-emitting diodes," *Optics Express*, vol. 28, no. 1, p. 665, 2020.

[2] R. T. Velpula, B. Jain, H. Q. T. Bui et al., "Improving carrier transport in AlGaN deep-ultraviolet light-emitting diodes using a strip-in-a-barrier structure," *Applied Optics*, vol. 59, no. 17, p. 5276, 2020.

[3] Y. Chen, C. Haller, W. Liu, S. Y. Karpov, J.-F. Carlin, and N. Grandjean, "GaN buffer growth temperature and efficiency of InGaN/GaN quantum wells: the critical role of nitrogen vacancies at the GaN surface," *Applied Physics Letters*, vol. 118, no. 11, Article ID 111102, 2021.

[4] B. Damilano and B. Gil, "Yellow–red emission from (Ga, In)N heterostructures," *Journal of Physics D Applied Physics*, vol. 48, no. 40, Article ID 403001, 2015.

[5] G. Martin, A. Botchkarev, A. Rockett, and H. Morkoç, "Valence-band discontinuities of wurtzite GaN, AlN, and InN heterojunctions measured by x-ray photoemission

spectroscopy," *Applied Physics Letters*, vol. 68, no. 18, pp. 2541–2543, 1996.

[6] F. Bernardini, V. Fiorentini, and D. Vanderbilt, "Spontaneous polarization and piezoelectric constants of III-V nitrides," *Physical Review B: Condensed Matter*, vol. 56, no. 16, pp. 10024–R10027, 1997.

[7] R. A. Arif, H. Zhao, and N. Tansu, "Type-II ingan-ganas quantum wells for lasers applications," *Applied Physics Letters*, vol. 92, Article ID 011104, 2008.

[8] H. Zhao, R. A. Arif, and N. Tansu, "Self-consistent gain analysis of type-II "W" InGaN–GaNAs quantum well lasers," *Journal of Applied Physics*, vol. 104, Article ID 043104, 2008.

[9] L. Han, K. Kash, and H. Zhao, "Designs of blue and green light-emitting diodes based on type-II InGaN-ZnGeN2 quantum wells," *Journal of Applied Physics*, vol. 120, no. 10, Article ID 103102, 2016.

[10] M. R. Karim and H. Zhao, "Design of InGaN-$ZnSnN_2$ quantum wells for high-efficiency amber light emitting diodes," *Journal of Applied Physics*, vol. 124, no. 3, Article ID 034303, 2018.

[11] A. Gorai, "Near-infrared light emitting diodes based on the type-II InGaN-ZnSnN2/GaN quantum wells," *Optical Materials*, vol. 85, pp. 337–340, 2018.

[12] S.-H. Park, D. Ahn, B. H. Koo, and J. E. Oh, "Optical gain improvement in type-II InGaN/GaNSb/GaN quantum well structures composed of InGaN/and GaNSb layers," *Applied Physics Letters*, vol. 96, no. 5, Article ID 051106, 2010.

[13] S. L. Chuang and C. S. Chang, "k-p method for strained wurtzite semiconductors," *Physical Review B: Condensed Matter*, vol. 54, no. 4, pp. 2491–2504, 1996.

[14] S.-H. Park and S. L. Chuang, "Piezoelectric effects on electrical and optical properties of wurtzite GaN/AlGaN quantum well lasers," *Applied Physics Letters*, vol. 72, no. 24, pp. 3103–3105, 1998.

[15] D. Ahn, "Theory of non-Markovian optical gain in quantum-well lasers," *Progress in Quantum Electronics*, vol. 21, no. 3, pp. 249–287, 1997.

[16] S.-H. Park, S. L. Chuang, J. Minch, and D. Ahn, "Intraband relaxation time effects on non-Markovian gain with many-body effects and comparison with experiment," *Semiconductor Science and Technology*, vol. 15, no. 2, pp. 203–208, 2000.

[17] S.-H. Park, D. Ahn, and S. L. Chuang, "Electronic and optical properties of ${\rm a}$- and ${\rm m}$-plane wurtzite InGaN–GaN quantum wells," *IEEE Journal of Quantum Electronics*, vol. 43, no. 12, pp. 1175–1182, 2007.

[18] W. Braun, P. Dowd, C.-Z. Guo et al., "Strained InGaAs/GaPAsSb heterostructures grown on GaAs (001) for optoelectronic applications in the 1100–1550 nm range," *Journal of Applied Physics*, vol. 88, no. 5, pp. 3004–3014, 2000.